On Simulating Concurrent Flame Spread in Reduced Gravity by Reducing Ambient Pressure

Maria Thomsen[a,*], Carlos Fernandez-Pello[a], David L. Urban[b], Gary A. Ruff[b], Sandra L. Olson[b]

[a]*Department of Mechanical Engineering, University of California - Berkeley, Berkeley, CA, 94720, USA*
[b]*NASA Glenn Research Center, Cleveland, OH, 44135, USA*

Abstract

The flammability of combustible materials in spacecraft environments is of importance for fire safety applications because the environmental conditions can greatly differ from those on earth, and a fire in a spacecraft could be catastrophic. Moreover, experimental testing in spacecraft environments can be difficult and expensive, so using ground-based tests to inform microgravity tests is vital. Reducing buoyancy effects by decreasing ambient pressure is a possible approach to simulate a spacecraft environment on earth. The objective of this work is to study the effect of pressure on material flammability, and by comparison with microgravity data, determine the extent to which reducing pressure can be used to simulate reduced gravity. Specifically, this work studies the effect of pressure and microgravity on upward/concurrent flame spread rates and flame appearance of a burning thin composite fabric made of 75% cotton and 25% fiberglass (Sibal). Experiments in normal gravity were conducted using pressures ranging between 100 and 30 kPa and a forced flow velocity of 20 cm/s. Microgravity experiments were conducted during NASA's Spacecraft Fire Experiment (Saffire), on board of the Orbital Corporation Cygnus spacecraft at 100 kPa and an air flow velocity of 20 cm/s. Results show that reductions of ambient pressure slow the flame spread over the fabric. As pressure is reduced, flame intensity is also reduced. Comparison with the concurrent flame spread rates in microgravity show that similar flame spread rates are obtained at around 30 kPa. The normal gravity and microgravity data is correlated in terms of a mixed convection non-dimensional parameter that describes the heat transferred from the flame to the solid surface. The correlation provides information about the similitudes of the flame spread process in variable pressure and reduced gravity environments, providing guidance for potential on-earth testing for fire safety design in spacecraft and space habitats.

Keywords: Flame spread rate, low pressure, environmental conditions, microgravity

*Corresponding author. Fax +1 510 642 1850
Email address: maria.thomsen@berkeley.edu (Maria Thomsen)

May 11, 2018

1. Introduction

Flame spread is one of the fire processes utilized to determine the flammability of solid combustible materials [1, 2]. For example, NASA relies on an upward flame spread test to screen materials to be used in spacecraft cabins [3]. Because a fire in a spacecraft would be catastrophic, it is critical to understand and predict fire spread behavior. Furthermore, spacecraft cabin environments are very different to those encountered in earth, they are in microgravity and low velocity flows induced by the spacecraft ventilation, and potentially, low pressure (~60 kPa) and elevated oxygen concentration (~34%) [4]. The latter conditions are referred to as Space Exploration Atmospheres (SEA) and are designed to reduce preparation time for space walks, while keeping the partial pressure of oxygen constant [5] and still hospitable to human habitation. Fire spread has been studied extensively [2, 6–11], and over the years, researchers have investigated the differences between flame spread in normal gravity (1g) and microgravity by looking at the effects of different variables such as geometry, low flow velocities, type of fuel, etc. [6, 12–18]. However, terrestrial microgravity testing is expensive and difficult: access to ground-based facilities such as drop towers or parabolic flights is restricted, the duration of the microgravity conditions provided is limited to a few seconds, and there are multiple safety limitations. For this reason, there is still a lack of information regarding the flame spread behavior under these conditions.

To expand the knowledge of flame spread behavior in spacecraft environments, NASA has embarked in a research project, the Spacecraft Fire Experiment (Saffire) [19], aimed to conduct flame spread tests of varied sizes and materials in an un-manned spacecraft, the Cygnus spacecraft by Orbital Sciences. The spacecraft is an autonomous cargo supply to the International Space Station (ISS). After separating from the ISS, the Cygnus would normally deorbit and burn up in the atmosphere. Instead, large scale fire tests or numerous small scale fire tests can be conducted prior to deorbitting, alleviating crew safety concerns. This approach is novel because it allows for significantly different experiments, using equipment that would have been otherwise been discarded. The work presented here has been conducted under the overall umbrella of the Saffire project.

Conducting experiments in a spacecraft is difficult and costly, thus it is relevant to study the possibility of simulating reduced gravity experiments on earth. A possible approach is to reduce pressure, and consequently density, to reduce gravity effects. Several studies have taken advantage of the changes in buoyancy resulting from reducing pressure to simulate conditions encountered in microgravity [20–23]. Nakamura et al. [21] studied flame spread over electric wires in low pressure environments and found that the flame shape in low pressure is similar to that observed in microgravity. Fereres et al. [23] studied numerically solid fuel pilot ignition similarities between microgravity and low pressure environments. They found that at low flow velocities ignition in microgravity could be approximated by reducing ambient pressure below 50 kPa.

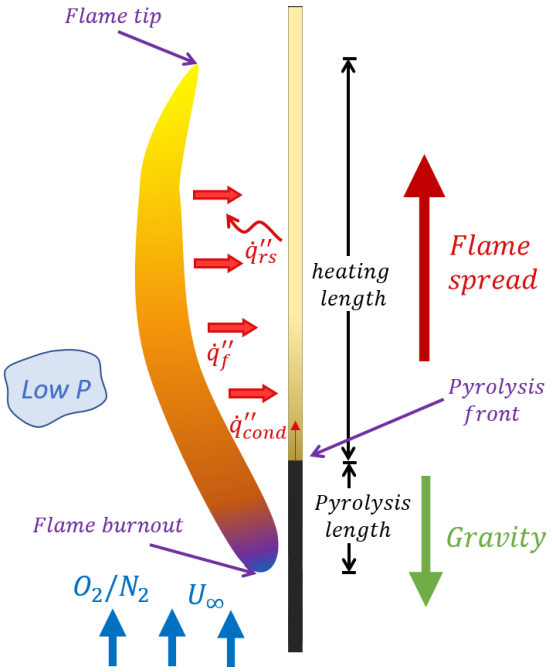

Figure 1: Diagram of a concurrent flame spread over a thin sample.

In the particular case of concurrent flame spread, reducing the ambient pressure (and density), thickens the boundary layer, moving the flame further form the surface, reducing heat transfer to the solid [24] (Fig. 1) . Consequently, the rate of flame spread is reduced, both because the reduced heat flux on the surface and a reduction in the flame length [25]. A similar effect on the flame characteristics and the spread rate is obtained by reducing the flow velocity. This is relevant because the primary constraints to reproduce flame spread in spacecraft environments in normal gravity is that the low flow velocities encountered in spacecraft (~0.1-0.2 m/s) cannot be attained in normal gravity because the buoyant flow (~0.4 m/s) overwhelms the forced flow. Thus, it seems possible that concurrent flame spread in reduced gravity, low velocity flows, could be at least partially

simulated in reduced pressure, low velocity flows. Verifying this hypothesis is the objective of this work.

In this study, the concurrent flame spread over a thin cotton/fiberglass composite fabric (Sibal) was investigated under normal gravity and varied reduced ambient pressure environments. This fabric was selected to compare the results with actual microgravity tests, particularly those of the Saffire experiments [19]. Other studies relevant to the present work are those of Zhao et al. [26] that studied the effect of forced flow and microgravity on flame development and concurrent flame spread for a similar fabric. Johnston et al. [27] that studied upward flame spread on long thin Sibal fabric. Olson et al. [28] that studied Sibal burning in an upward configuration focusing in the flame growth and pressure rise while also burning large-scale samples (~1 m long). These studies, together with the present one, provide further understanding on the effect of gravity and ambient pressure on the flame spread process over thin materials.

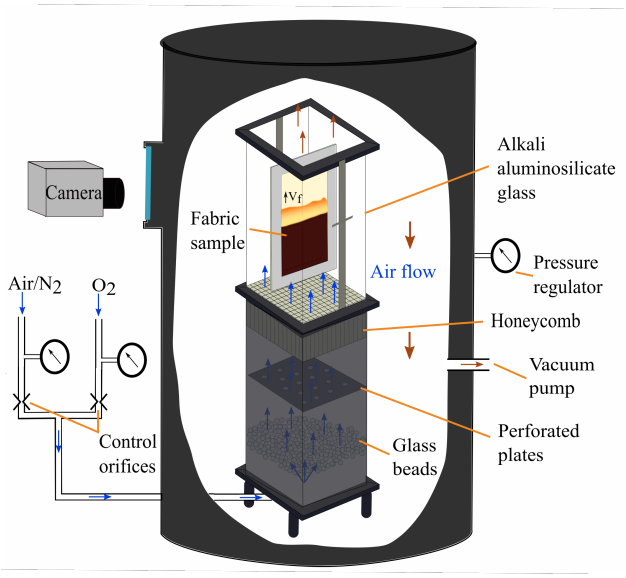

Figure 2: Schematic of experimental apparatus.

2. Experiments

The normal gravity experiments were conducted in an apparatus previously developed to study the flammability of solid combustible materials under varied ambient conditions [20]. The apparatus consists of a laboratory scale combustion tunnel that is inserted in a pressure chamber (Fig. 2). The tunnel has a 125 mm by 125 mm cross section and is 600 mm in total length. The first 350 mm section of the duct serves as a flow straightener, the other 250 mm segment of the duct is used as the test section. The side walls of the test section (normal to the plane of the samples) are made of clear polycarbonate. The walls parallel to the sample are 0.56 mm thick alkali-aluminosilicate glass. A single layer of a fabric is placed vertically at the midplane of the test section with both sides exposed to the flow. The fabric ignition is induced with a 29-gage Kanthal wire braided along the upstream edge of the fabric (see Fig. 3). The igniter is energized using a controlled current power supply (BK Precision 1785) set to deliver 40 W for 3 s.

The fabric sample was selected to match one of the materials tested in the Saffire I and II microgravity experiments [19]. The fabric, Sibal, is a blend made of 75% by mass of cotton and 25% of fiberglass, and has an overall area density is 18.0 mg/cm^2. The non-combustible fiberglass in the matrix of the fabric provides structural integrity and prevents the fabric from curling or cracking while burning. The Sibal samples tested were 150 mm long by 50 mm wide, smaller than the ones used during the Saffire test. The sample was held in between two identical stainless-steel frames of 200 mm by 125 mm and 0.4 mm thick. Each frame had an identical rectangular opening the size of the sample to serve as the test area. The tests were conducted in air under pressures of 100, 70, 40, and 30 ± 2 kPa. Compressed house air was supplied through critical nozzles (O'Keefe Controls) while constantly evacuating to maintain constant the pressure inside the chamber. The chamber pressure was controlled by a high-capacity vacuum generator (Vaccon JS-300) and a mechanical vacuum regulator. After metering, the supply line passed through a bulkhead in the pressure chamber and delivered directly to the inlet of the test duct located in the bottom part. This process ensured that flow through the duct was continually fresh and maintained at a constant mass flow rate.

The chamber pressure was monitored constantly with an electronic pressure transducer (Omega Engineering, Inc. PX303-015A5V). The forced flow was fixed to 20 cm/s in all the test. The direction of the flow was upward so that the spread of the flame was in the concurrent configuration. Once the sample was in position, the chamber was sealed to adjust the system to the desired conditions. Two 9000 lumen LED were installed with an operating electronic circuit to act as a strobe light to visualize and measure during the same experiment flame spread rates and the flame appearance. The ignition and subsequent flame spread were video recorded

with a resolution of 1280 by 720 at 59 frames per second using a Nikon D3200 camera to track the pyrolysis front. A second camera (Sony RX10-III) was used to record videos of visible flame length with a resolution of 1280 by 720 at 59 frames per second. For each test condition, between three and five replicate experiments were conducted to address the experimental uncertainty.

The microgravity experiments were conducted in the Microgravity Science Glove-box aboard the ISS [26] and the Orbital Corporation Cygnus spacecraft (Saffire I and II) [19]. The reader is referred to those publications for details of the respective experiments.

3. Results

The normal gravity concurrent flame spread was investigated under different ambient pressures. The primary data collected were burnout, pyrolysis front and flame tip positions. Fig. 3 shows two representative frames of the flame spreading over the sample. Fig. 3a displays the sample with the strobe light on and shows the pyrolysis front. Fig. 3b is with the strobe light off and shows the flame burnout and flame tip. Here, the position of the pyrolysis front was defined as the point where the fabric is first visibly blackened. The burnout front position was defined as the upstream edge of the flame, which coincides with where the flame begins receding. During each test, after ignition is achieved, the flame spreads uniformly along the surface of the sample. The pyrolysis front had an inverted "U" shape in all tests. The flame tip had a flickering inverted "V" shape. The flame flickering appears to decrease as the pressure is decreased. Usually, after ignition of the sample, a short initial period of laminar flame spread was observed, followed by the flame transitioning to a turbulent flame. As the flame spreads over the fabric it consumes most of the cotton, leaving behind the fiberglass mesh and some smoldering cotton residue (bottom of Fig. 3b).

A characteristic result of the time evolution of the pyrolysis and burnout fronts is presented in Fig. 4 for an ambient pressure of 40 kPa. Also included is the evolution of the pyrolysis length. For validation purposes the data of Olson et al. [28] is also presented in Fig. 4. Note that although the length of the samples in Ref. [28] are larger than in the present tests (1 m vs 0.15 m), both tests show very similar data during the initial part of the spread of the flame, with the flame spread rate increasing with time initially and then eventually reaching steady state for the larger samples. The results show that the samples used in the present experiments were not long enough for the flame spread to reach steady state, although the pyrolysis front approaches steady spread faster than the burnout front.

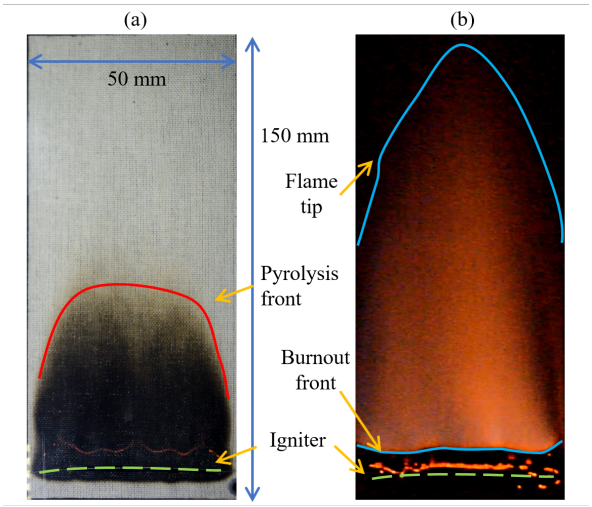

Figure 3: Front view showing two representative frames with the (a) pyrolysis front, and (b) flame tip and burnout front.

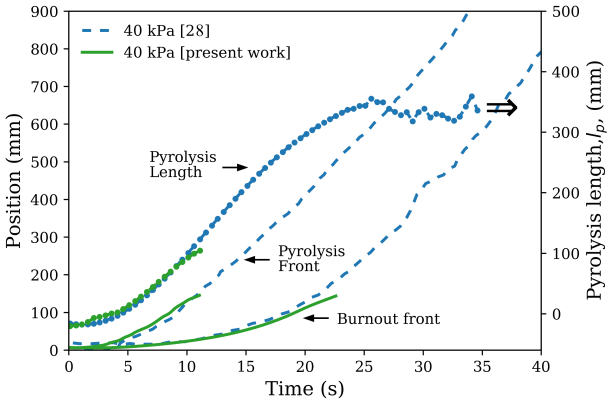

Figure 4: Location of the pyrolysis front and burnout front position, as well as the pyrolysis length, as a function of time for an ambient pressure of 40 kPa.

Fig. 5 shows the progress of the pyrolysis front and burnout front for pressures ranging from 100 to 30 kPa. It is seen that as pressure is reduced the spread of the flame is slower. During most of the tests, the flame is still accelerating as it spreads over the solid. However, as pressure is reduced, the pyrolysis front and flame burnout front begin to stabilize faster. Similar results were also reported by Olson et al. [28] with longer sam-

ples. It is seen that the average total burn time for the 100 kPa initial pressure was 13.2 s, significantly smaller when compared to the average 43.7 s obtained at about 30 kPa. For comparison purposes, the evolution of the pyrolysis and burnout fronts from the Saffire II experiments [19] are included in Fig. 5. It is seen that as the ambient pressure is reduced, the pyrolysis and burnout front data approaches the microgravity data.

The flame brightness is also affected by pressure changes, becoming weaker as pressure is reduced. In these conditions, the flame changes from a bright yellow/orange to a faint purple/orange color, as shown Fig. 6. Visible flame height is also reduced, although for the lower pressures the flame tip becomes very diffuse and hard to define. Also, as the pressure is reduced, the flame appearance became similar to what was observed during the Saffire microgravity experiments. The photographs of the Saffire tests could not be include in Fig. 6 to compare with the normal gravity ones because they are too dark and difficult to reproduce here.

The progress of the pyrolysis front is often used to determine the flame spread rate. Fig. 7 shows the average flame spread rate as a function of ambient pressure as obtained from the pyrolysis front data of Fig. 5. Because of the size of the samples, and the accelerative characteristics of the flame, an averaged spread rate over the last 50 mm of the sample is presented so that the data are closer to the steady state value and transient effects are minimized. For comparison, the flame spread rate data of Saffire I and II [19] and the microgravity data of Zhao et al. [26] are also included. It is seen that in normal gravity the flame spread rate decreases from 41.8 to 5.4 mm/s as the ambient pressure decreased from 100 to 30 kPa, at which point the flame spread rate was similar to the microgravity value in the Saffire test, 2.03 mm/s.

An important parameter for concurrent flame spread is the pyrolysis length (Fig. 1) because it determines the flame length and consequently the heat transferred from the flame to the solid. The variation of the pyrolysis length with pressure is also included in Fig. 7. The pyrolysis length is obtained toward the end of the test when it approaches steady state. It is seen that in normal gravity the pyrolysis length decreases with decreasing ambient pressure. As pressure is reduced to 30 kPa, the pyrolysis length in normal gravity approaches that in microgravity. Both results are an indication that concurrent flame spread in low pressure and normal gravity, may have similar characteristics as that in reduced gravity. It should be kept in mind however, that the total pressure reduction necessary to see these similarities will vary depending of the material and environmental conditions used.

4. Discussion: Effect of Buoyancy

To understand the observed dependence of the flame spread rate on pressure it is helpful to use a simplified analysis of flame spread as that developed by Fernandez-Pello [9]. The analysis provides an analytical equation for the concurrent flame spread rate as:

$$V_f = l_h \left(\frac{\rho_s c_s s (T_p - T_o)}{\dot{q}''_{fc} + \dot{q}''_{fr} - \dot{q}''_{rs}} + \frac{Cx}{U_m} t_{chem} \right)^{-1} \qquad (1)$$

where l_h is the heated length, $\dot{q}''_{fc}$, represents the convective heat flux at the solid surface, $\dot{q}''_{fr}$ is the flame radiant flux, $\dot{q}''_{rs}$ the re-radiation from the solid, U_m the mixed flow (forced and free) velocity, t_{chem} the chemical time, ρ_s and c_s are the solid density and specific heat and s is the solid thickness. T_p and T_o represent the pyrolysis and initial temperatures of the solid. The first term in Eq. 1 describes the heat transfer mechanisms controlling the flame spread process and the second term the gas phase chemical kinetic. The contribution of the chemical kinetics term is small until the pressure becomes of the order of 30 kPa [29]. Assuming that the radiant flux from the flame approximately balances the surface re-radiation, then the flame spread rate is primarily determined by the product of the flame heated length, l_h, and the convective heat flux, $\dot{q}''_{fc} = h(T_f - T_p)$, with h representing the convective heat transfer coefficient and T_f is the flame temperature.Flame temperature is not strongly dependent on ambient pressure until the chemical time starts to become larger than the physical time, thus it is considered constant in the range of the present experiments. The heating length is related to the pyrolysis length as $l_h \sim C l_p$ [9]. Under these conditions the flame spread rate becomes

$$V_f \approx l_p \left[\frac{h(T_f - T_p)}{\rho_s c_s s (T_p - T_o)} \right] \qquad (2)$$

From Eq. 2 it is seen that the flame spread rate is proportional to the convective heat transfer coefficient at the solid surface, which is a function of the problem parameters. For a mixed flow, forced and free, as that of the normal gravity experiments the average convective heat transfer coefficient can be expressed in terms of the Reynolds number and the Grashof number as [30]:

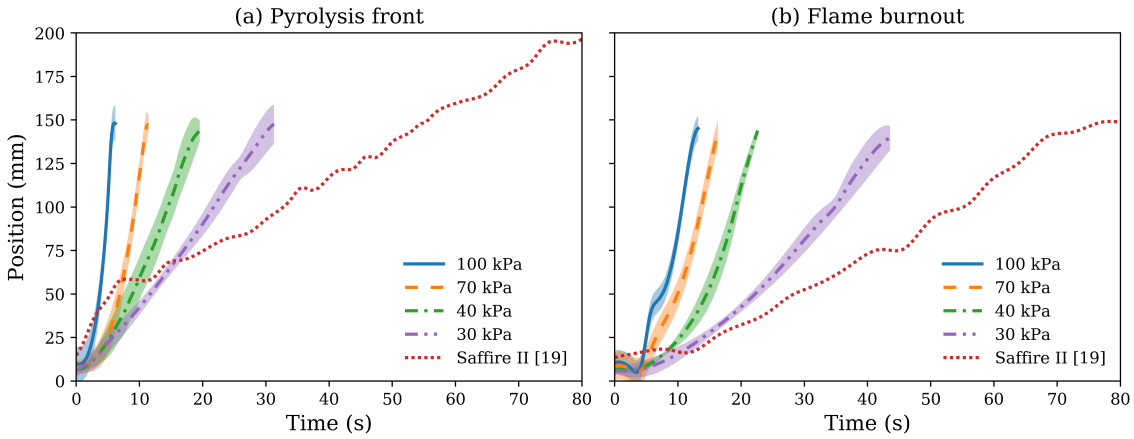

Figure 5: Time evolution of the (a) pyrolysis front position and (b) flame burnout position for different ambient pressures and the Saffire II experiment [19].

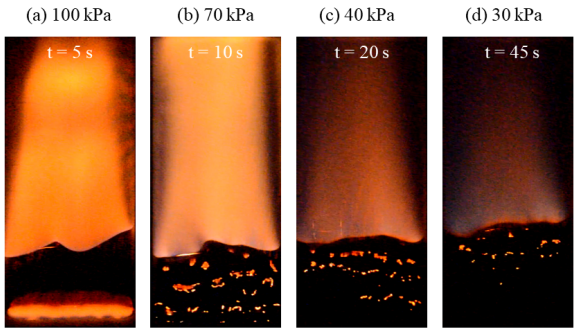

Figure 6: Effect of ambient pressure on flame appearance.

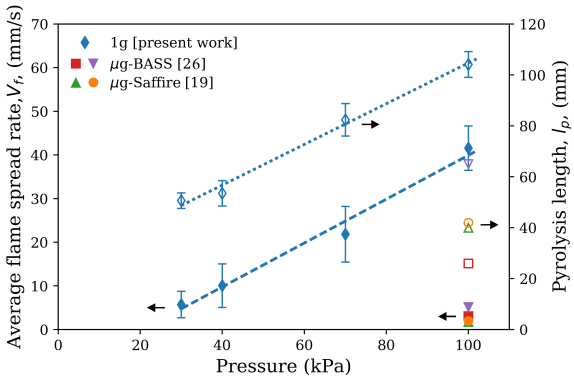

Figure 7: Measured average flame spread rate (filled symbols) and pyrolysis length (hollowed symbols) as a function of ambient pressure.

$$h = C\frac{k}{l_p}\left(Re^4 + Gr^2\right)^{1/8} Pr^{1/3} \quad (3)$$

$$= C\frac{k}{l_p} Re^{1/2}\left(1 + \frac{1}{Fr^2}\right)^{1/8} Pr^{1/3} \quad (4)$$

where $Re = \rho U_f l_p/\mu$, $Gr = g\beta\Delta T l_p^3\rho^2/\mu^2$, and $Fr = Re^2/Gr = U_f^2/gl_p$. Here l_p is the pyrolysis length which is taken as the solid surface characteristic length in the flow direction, U_f is the forced gas velocity, μ is the dynamic viscosity, ρ is gas phase density, β is the coefficient of thermal expansion and g is gravity level. It is seen that the heat flux at the surface is determined by a mix flow non-dimensional parameter that is a combination of the Grashof and Reynolds numbers. Substituting Eq. 4 into Eq. 2, a relation is obtained between the flame spread rate and the problem parameters as shown in Eq. 5.

$$V_f \propto P^{1/2} l_p^{1/2} U_f^{1/2}\left(1 + \frac{g^2 l_p^2}{U_f^4}\right)^{1/8} \quad (5)$$

The above relation shows that at low forced flow velocities, like in the 1g experiments, the heat transfer from the flame to the surface is dominated by natural convection ($h \propto Gr^{1/4} \propto g^{1/4}P^{1/2}l_p^{3/4}$) so $V_f \propto g^{1/4}P^{1/2}l_p^{3/4}$ as in upward flame spread over a thermally thin fuel [9]. At large flow velocities or low gravity, like in the μg tests, by forced convection ($h \propto Re^{1/2} \propto P^{1/2}l_p^{1/2}U_f^{1/2}$) so $V_f \propto P^{1/2}l_p^{1/2}U_f^{1/2}$ as in forced flow flame spread over a thermally thin fuel [9]. It should be noted that the predicted dependence of the concur-

rent flame spread on pressure of Eq. 5 is the same as that obtained by Olson et al. [11] in their correlation of available data on concurrent flame spread over thin fuels. The predicted dependence of the flame spread rate on the forced flow velocity is not linear as found by Olson et al. [11], although the product $l_p^{1/2}U_f^{1/2}$ is approximately linear.

Equation 5 can be used to plot the normal gravity, low pressure data and the microgravity, normal pressure data along a common variable. Plotting the flame spread rate data of Fig. 7 in terms of Eq. 5, as in Fig. 8, it is seen that as the pressure is reduced the flame spread rate decreases and approaches that obtained in microgravity. Also, flame spread rate as a function of pressure and gravity, agrees well with what is expected from a scaling analysis using Grashof number as reported by [22]. The pyrolysis length can also be correlated using the above approach, as shown in Fig. 8. It is seen that a similar trend is observed for the pyrolysis length, and that the normal gravity data aligns well with that obtained in microgravity, at least for the Saffire data.

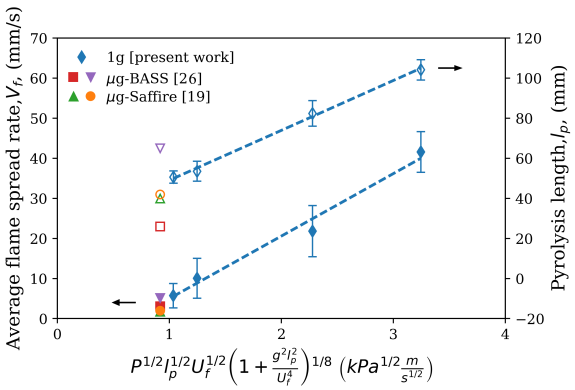

Figure 8: Measured average flame spread rate (filled symbols) and pyrolysis length (hollowed symbols) as a function of the relation to P and g.

It should be noted that a similar alternative approach to correlate the flame spread data in terms of the problem parameters can be made by defining a mixed flow gas velocity that when applied in a forced flow boundary layer analysis will produce a boundary layer of the same thickness to that of the mixed flow. This approach is logical since the heat transfer coefficient is directly related to the boundary layer thickness, δ, through $h = k/\delta$, and the boundary layer thickness is directly related to the gas flow velocity. Following this approach, the mixed convective flow velocity can be obtained by equating the boundary layer thickness for a forced flow ($\delta_f = l_p Re^{1/2} Pr^{1/3}$) with that for a mixed convective flow ($\delta_m = l_p (Re^4 + Gr^2)^{-1/8} Pr^{1/3}$), which gives

$$U_m = \frac{P}{P_0} U_f \left(1 + \frac{g^2 l_p^2}{U_f^4}\right)^{1/4} \tag{6}$$

Substituting this equivalent forced flow velocity, U_m, of Eq. 6 for the forced flow velocity, U_f, in Eq. 5 and setting $g = 0$, the resulting flame spread rate would be that of a forced flow with a velocity equal to that of the mixed flow. The correlation of the data of Fig. 7 in terms of the mixed flow velocity as obtained with Eq. 5 is given in Fig. 9. It is seen that the microgravity data can also be correlated well using this approach. It is also seen that the flame spread is linearly proportional to the mixed flow velocity, in agreement with theoretical predictions [9] and with experimental measurements of concurrent flame spread over paper [24].

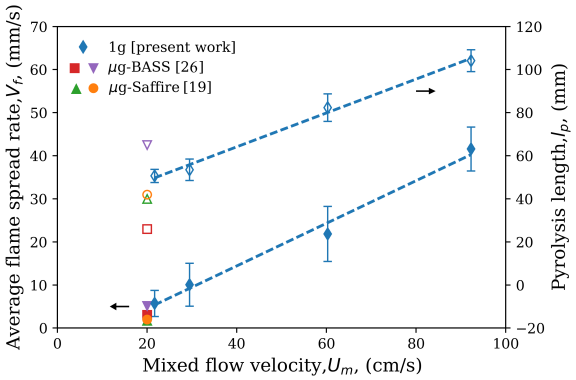

Figure 9: Measured average flame spread rate (filled symbols) and pyrolysis length (hollowed symbols) as a function of the mixed flow velocity from Eq. 6.

The results of Fig. 8 and 9 are relevant because they indicate that the concurrent flame spread over Sibal in a microgravity environment can be approximately simulated by reducing the ambient pressure to levels of the order of 30 kPa. However, at those low-pressure levels chemical kinetic effects start to become important in the flame spread process and may give inaccurate predictions for other fuels and environmental conditions, particularly oxygen concentration. It is also relevant that different gravity levels, such as in the Moon or Mars, can be also simulated with this flame spread formulation. At those gravity levels the simulation pressure would be higher, and consequently the chemical kinetic effects would be reduced.

5. Conclusion

The concurrent flame spread rate and flame appearance of a thin composite fabric (Sibal) burning in different environments have been study under reduced ambient pressure. It has been found that as pressure is reduced, the flame spread rate over a thin fabric is also reduced. Flame intensity is also weakened resulting in dimmer blue-purple flames. As ambient pressure is reduced to around 30 kPa the flame spread rate approaches that observed in microgravity. The correlation of the flame spread rate data in terms of a mixed flow parameter that includes gravity and pressure suggests that reduced pressure can be used to simulate untested levels of gravity conditions.

It should be kept in mind, however, that variations in ambient pressure will affect flame chemistry. For a constant oxygen concentration, as total ambient pressure is reduced there is a subsequent reduction in the partial pressure of oxygen and flame temperature [31]. Additionally, lower pressure environments result in an increase in the mean free path between molecules ($\lambda \propto 1/P$), therefore reducing the number of collisions in the reaction zone and thickening the flame sheet [32]. The combined effect of reduced partial pressure of oxygen and a larger mean free path between molecules, slows down the chemical reactions in the gas phase, affecting the heat provided by the flame to the unburned solid and therefore reducing the flame spread rate. Thus, care should be taken interpreting and applying these results, particularly because eventually low pressure will affect the chemical kinetics of the process.

6. Acknowledgments

This research is supported by NASA Grant NNX12AN67A. Maria Thomsen would like to acknowledge the support BecasChile through the scholarship program Becas de Doctorado en el extranjero convocatoria 2014 (#72150022). The authors would like to thank Saul Pacheco, Grace Mendoza, Miguel Soto, and Runbiao Wei for their contributions conducting part of the experiments.

References

[1] F. A. Williams, P. Combust Inst. 16 (1977) 1281–1294.
[2] J. Quintiere, Fire Mater. 5 (1981) 52–60.
[3] National Aeronautics and Space Administration, NASA-STD-6001B Flammability, Offgassing, and Compatibility Requirements and Test Procedures, Technical Report I, Washington, DC, 2011.
[4] K. E. Lange, A. T. Perka, B. E. Duffield, F. F. Jeng, Bounding the Spacecraft Atmosphere Design Space for Future Exploration Missions, Technical Report June, 2005.
[5] T. Hirano, in: Proc. 5th AOSFST, pp. 40–55.
[6] S. Bhattacharjee, R. A. Altenkirch, N. Srikantaiah, M. Vedhanayagam, Combust. Sci. Technol. 69 (1990) 1–15.
[7] A. C. Fernandez-Pello, T. Hirano, Combust. Sci. Technol. 32 (1983) 1–31.
[8] G. H. Markstein, J. De Ris, P. Combust. Inst. 14 (1973) 1085–1097.
[9] C. Fernandez-Pello, in: Combustion Fundamentals of Fire, Academic Press Limited, cox, geoff ed., 1994, pp. 31–100.
[10] I. S. Wichman, Prog. Energ. Combust. 18 (1992) 553–593.
[11] S. L. Olson, G. A. Ruff, F. J. Miller, in: 38th International Conference on Environmental Systems, San Francisco, California, pp. 1–8.
[12] S. L. Olson, P. V. Ferkul, J. S. T'ien, P. Combust. Inst. 22 (1989) 1213–1222.
[13] S. L. Olson, Combust. Sci. Technol. 76 (1991) 233–249.
[14] S. L. Olson, F. J. Miller, P. Combust. Inst. 32 (2009) 2445–2452.
[15] M. Kikuchi, O. Fujita, K. Ito, A. Sato, T. Sakuraya, Symposium (International) on Combustion 27 (1998) 2507–2514.
[16] A. Umemura, M. Uchida, T. Hirata, J. Sato, P. Combust. Inst. 29 (2002) 2535–2543.
[17] P. V. Ferkul, S. L. Olson, M. C. Johnston, J. S. T'ien, in: 8th U. S. National Combustion Meeting, Park City, Utah, pp. 1–12.
[18] A. F. Osorio, K. Mizutani, C. Fernandez-Pello, O. Fujita, P. Combust. Inst. 35 (2015) 2683–2689.
[19] P. Ferkul, S. Olson, D. L. Urban, G. A. Ruff, J. Easton, J. T'ien, Y. T. T. Liao, C. A. Fernandez-pello, J. L. Torero, C. Eigenbrod, G. Legros, N. Smirnov, O. Fujita, S. Rouvreau, B. Toth, G. Jomaas, in: Proc. 47th International Conference on Environmental Systems, July, Charleston, South Carolina, pp. 1–10.
[20] M. Thomsen, D. C. Murphy, C. Fernandez-pello, D. L. Urban, G. A. Ruff, Fire Safety J. 91 (2017) 259–265.
[21] Y. Nakamura, N. Yoshimura, H. Ito, K. Azumaya, O. Fujita, P. Combust. Inst. 32 (2009) 2559–2566.
[22] J. Kleinhenz, I. I. Feier, S. Y. Hsu, J. S. T'ien, P. V. Ferkul, K. R. Sacksteder, Combust. Flame 154 (2008) 637–643.
[23] S. Fereres, C. Fernandez-Pello, D. L. Urban, G. A. Ruff, Combust. Flame 162 (2015) 1136–1143.
[24] H. T. Loh, C. Fernandez-Pello, Twentieth Symposium (International) on Combustion (1984) 1575–1582.
[25] P. V. Ferkul, J. S. T'ien, Combust. Sci. Technol. 99 (1994) 345–370.
[26] X. Zhao, Y. T. T. Liao, M. C. Johnston, J. S. T'ien, P. V. Ferkul, S. L. Olson, P. Combust. Inst. 36 (2017) 2971–2978.
[27] M. C. Johnston, J. S. T'Ien, D. E. Muff, X. Zhao, S. L. Olson, P. V. Ferkul, Fire Safety J. 71 (2015) 279–286.
[28] S. L. Olson, S. A. Gokoglu, D. L. Urban, G. A. Ruff, P. V. Ferkul, P. Combust. Inst. 35 (2015) 2623–2630.
[29] S. McAllister, C. Fernandez-Pello, D. Urban, G. Ruff, Combust. Flame 157 (2010) 1753–1759.
[30] C.-P. Mao, A. C. Fernandez-Pello, P. J. Pagni, J Heat Transfer 106 (1984) 304–309.
[31] I. Glassman, R. A. Yetter, Combustion, 4 ed., Academic Press, New York, 2008.
[32] H. D. Ross, in: H. D. Ross (Ed.), Microgravity Combustion: Fire in Free Fall, 2001, pp. 1–33.